Biomedical Applications of Antimicrobial Metal-Organic Frameworks

Rob Marusko, Dr. Eubank

I. Abstract

In recent years, the field of metal-organic frameworks has seen dramatic increases in exploration. Metal-organic frameworks, commonly referred to as MOFs, have been shown to be excellent candidates for the storage of fuels (e.g., methane and acetylene), capture of gasses (e.g., hydrogen or carbon dioxide), and catalyzing reactions. With more than 20,000 different MOFs being reported and studied within the past decade, the focus of their applications has been constantly broadening and shifting. One area that has burgeoned more recently is the biomedical applications of these frameworks (particularly as antimicrobial agents) which has direct correlations and implications to the fields of medicine and dentistry, the particular interest of this project. One purpose of this particular project was to study the design and synthesis of metal-organic frameworks, in general, and tailor them toward biomedical applications, specifically. Upon the design and synthesis of suitable materials (e.g., biocompatible or bioactive), state-of-the-art structural analysis techniques (e.g., powder and single-crystal x-ray diffraction) were utilized for structure and phase confirmation. The expected bioactive materials were then evaluated for their antimicrobial properties. These materials are well-known for their modularity, and the explored structures were tailored to access/include different moieties (e.g., metal/ligand substitution, functionalization, etc.) with hopes of contributing to increased antimicrobial effectiveness.

II. Introduction

The long term objective of this study was to develop a biologically safe, antimicrobial metal-organic framework to be used in conjunction with dental implants. Specifically, this framework would be employed to reduce or prevent the occurrence of peri-implantitis in at-risk patients. Peri-implantitis encompasses the criteria of peri-mucositis and the additional loss of osseous support. The prevalence of this issue is exemplified well in a study of 280 periodontists, where it was found that up to 25% of their patients have peri-implantitis, and up to 10% of implants must be removed due to peri-implantitis.[1] Furthermore, it was found that only 5.1% of all practitioners believe that any treatment currently available is effective.[1] The treatments currently available prioritize decontamination of the infected site, and include nonsurgical procedures with or without local-release antibiotics, surgeries that include flap debridement, and regenerative procedures such as bone grafts with or without barrier membranes.[2] Despite the apparent diversity of approaches here, Two of the more complete reviews could not identify any one protocol as being more predictable or superior than the others in terms of treatment outcomes.[3,4] In evaluating these available treatments, it is of note that all of them are restorative rather than preventative. This is where the inspiration for this project came from, as the development of a preventative mechanism for peri-implantitis would save dental professionals time and would likewise save their patients time, money and discomfort.

Historically, bacterial infections play the most important role in the failure of dental implants. The bacteria which are associated with periodontitis and peri-implantitis are found to be similar, and the organisms most commonly related to the failure of an implant are the Gram-negative anaerobes.[5] These bacteria are organisms such as *Prevotella intermedia, Porphyromonas*

gingivalis, Aggregatibacter actinomycetemcomitans, Bacterioides forsythus, Treponema denticola, Prevotella nigrescens, Peptostreptococcus micros, and *Fusobacterium nucleatum*.[6] A number of different reviews on the oral microbiome support this data, indicating that these are all potential targets for antimicrobial testing.[2] With that in mind, a different bacteria was proposed for testing. *S. mutans* is a gram positive microbe that is found broadly within the healthy microbiome. A 2010 publication by Persson and his team discussed how this bacteria, while not harmful itself, is principally responsible for biofilm development on dental implants almost immediately after this placement. Without the adhesion of this biofilm, harmful bacteria are significantly impeded, if not inhibited, from binding to the implant and subsequently causing periimplantitis.[7,8] In light of this, it was decided to target *S. mutans* with the hope of preventing biofilm formation and eliminating the problem of periimplantitis before it even started. Targeting *S. mutans* also addressed how issues with non-pathogenic bacteria can be nonetheless catastrophic to oral and holistic health. For example, in addition to the challenges of gingival infections, there are a number of different sources of infection that can be detrimental to the structural integrity of teeth and implants. Some bacteria, while not harmful themselves, will oxidize titanium implants. Not only does this oxidation attack the integrity of dental implants, but it also causes dissolution of metal ions and particles in the oral environment.[9] This dissolution can trigger or contribute to the development of peri-implantitis at later stages. In addition to these non-harmful bacteria, there is an assortment of bacteria in the oral microbiome that result in gum loss, bone resorption, and dental caries.[10]

Although many metals and organic molecules are known to be antibacterial, if they are to be utilized for *in vivo* applications it was first necessary to ensure their biocompatibility. A publication by Wuttke, et. al. (2017) evaluated the safety of different metal-organic frameworks for diverse medical applications. The authors evaluated the effects of MOFs on human endothelial and mouse lung cells. Of particular interest, they validated specific MOFs for dental applications, i.e., multifunctional surface coatings of dental implants. While testing the frameworks against human gingival fibroblast cells, they found that biocompatibility varied significantly with structure composition.[2] However, they did confirm that several frameworks presented no adverse effects when introduced to human gingival fibroblast cells in particular.[11] In a more general sense, there is extensive data showing the applications of metal-organic frameworks in biomedicine, acting as a number of different agents.[12,13,14]

Knowing that several different frameworks were biocompatible, the next step was to explore antimicrobial properties of the metal-organic frameworks. While this characteristic is highly dependent on the composition of individual frameworks, previous research has validated that some of these structures can effectively inhibit bacterial growth. A project performed by Lu et. al. (2014) explored the properties of two novel silver-based MOFs. Their results indicated that both compounds exhibit leaching/degradation, resulting in slow release of Ag^+ ions, and that this slow release was excellent for long-term antimicrobial activities towards Gram-negative bacteria *Escherichia coli* and Gram-positive bacteria *Staphylococcus aureus*.[15] Additional studies have validated that this property is not limited to silver-based frameworks, with Cu, Zn, and Co being cited amongst many other frameworks with these properties.[16]

As the intention of this project was to produce a synergistic antimicrobial result between the metal and ligand of the experimental frameworks, it was not enough that the metal independently (Cu) was antimicrobial. In addition, it needed to be supported by an antimicrobial ligand.[17] While chelidonic acid is thought to be somewhat antimicrobial, it displayed little effectiveness against the target bacteria. In light of this, the modularity of these compounds was employed to

substitute chelidonic acid for different sulfonamides. A 2016 article by Borthagaray et. al. addressed metal-ion complexation as a strategy to improve antimicrobial effectiveness of drugs. This article talked about copper complexes which employed sulfonamide ligands and achieved biologically significant results. Sulfonamides are unique compounds which are "extensively used in medicine due to their antimicrobial properties and they present coordination versatility acting as monodentate ligands"[18] In particular, this study showed that all the Copper-sulfonamide complexes were active against S. aureus and E. coli but only the complexes with ligands having a five-membered heterocycle were more active than the free sulfonamides. It was then proposed that we attempt to use sulfonamides as branching ligands (exchanged for chelidonic acid) as well as using them as terminal ligands in place of pyridine. If crystal could be induced, the resulting product may have the potential to be significantly more biologically active. The work done by Borthagaray et. al. has been supported by additional projects, where modified toxicological and pharmacological properties have been observed when some of these sulfonamides are administered in the form of their metal complexes.[19]

To effectively use metal-organic frameworks in conjunction with dental implants, it is hypothesized that the frameworks may be able to be grown directly on the implants. While there is limited research exploring this specific functionalization, the work of Centrone et. al. (2010) found that polymer substrates can be functionalized with a MOF material (MIL-47), which was synthesized directly on polyacrylonitrile using microwave irradiation.[20] Additionally, work has been done adhering metal-organic frameworks to PVDF hollow fiber membranes[21] as well as one exceptionally promising article which used natural cotton and a layer-by-layer dip-coating technique to synthesize a homogenous, surface supported film composed of Cu based frameworks.[22] This, in conjunction with other literature, served as a basis for initiating studies of adhesion to titanium surfaces. This presented another avenue for exploration, which was explored extensively throughout this project.

III. Goals and objectives of this study

As referred to in the abstract, one purpose of this particular project was to study the design and synthesis of metal-organic frameworks, in general, and tailor them toward biomedical applications, specifically. Before beginning to explore the applications of these structures, it was incredibly important that they were fully understood and that the data gathered could be analyzed efficiently and effectively. Furthermore, it was crucial that an analysis of this data could be used to evaluate and alter structural properties. Initially, this project explored the antimicrobial effectiveness of two distinct frameworks, "RM1($C_{17}H_{14}Cu\ N_2\ O_7$) and RM2 ($C_{42}H_{36}Cu_2N_6O_{13}$)". Preliminary studies were conducted on the antimicrobial effectiveness of these frameworks, but issues with standardization of bacterial growth resulted in promising, but inconclusive data. This project first sought to identify whether or not these frameworks are significantly antimicrobial (through the screening of *S. mutans*), which had a direct influence on the focus of the rest of the project. The results of this testing, which are elaborated on below, led to the necessity of generating new frameworks through ligand exchange. As briefly discussed in the background above, sulfonamides were introduced into the frameworks in the place of with pyridine. This resulted in new frameworks, generically represented as $((Cu)_x(CDO)_y(Sulfonamide)_z)_n$ Previous work had shown that these structures could increase antimicrobial effectiveness of metal ion clusters when employed as terminal ligands. While working to improve the antimicrobial properties of these frameworks, their adhesive properties

on different surfaces (e.g., glass and titanium) were also explored. The results of all of these trials are discussed thoroughly throughout this report.

Materials and Methods

All chemicals were used as purchased. Single-crystal X-ray diffraction data was obtained from original paper (Eubank et. al.).[23] Novel framework single-crystal X-ray diffraction was performed by Dr. Khalil Abboud, Director of Single Crystal X-Ray Facilities at UF.

Powder X-ray diffraction data was collected on a Bruker D_2 Phaser CCD diffractometer at FSC.

Conditions for synthesis of different crystalline product varied significantly throughout the course of this project, typically in an attempt to modify the size, structure or crystallinity of a product. However, all trials employed a ratio of ethanol and DMF as the solvent. The most significant synthesis reactions are elaborated on here and displayed in tables.
Crystal synthesis of RM1 and RM2 both employed 0.04mmol of Cu^{2+} and 0.04mmol of chelidonic acid, as well as 0.1ml pyridine. The solvent ratio of DMF to ethanol varied, from pure DMF for RM2 to a 1:1 ratio for RM1. The solid reagents (Cu^{2+} and chelidonic acid) were always solubilized in DMF while sonicating before adding additional solvent. These conditions were expanded upon and modified in additional runs for anticipated new crystal formation, and the modifications are presented in the results section when discussed. Crystals were synthesized in a non-ramping oven at 80ºC.

Table 1. Condition Dependent Crystal Formation

Vial	M/L	Metal (in DMF)	Ligand (in DMF)	Dimethyl formamide	Ethanol	Pyridine	Notes
Cndtn 1	1.0 ml	0.5 ml	0.5 ml	1.0 ml	-	0.1 ml	80ºC for 24hrs
Cndtn 2	1.0 ml	0.5 ml	0.5 ml	0.5 ml	0.5 ml	0.1 ml	80ºC for 24hrs.
Cndtn 3	1.0 ml	0.5 ml	0.5 ml	0 ml	1.0 ml	0.1 ml	80ºC for 24hrs

Where Cndtn1 produced RM2, cndtn3 produced RM1, and cndtn2 produced a mixture of the two phases.

RM 31 followed the same conditions as RM2, but increased the pyridine from 0.1ml to 0.8ml.

Table 2 - Verification of Novel Framework, Known as RM31

Vial	M/L	M (in DMF)	L (in DMF)	DMF	EtOH	Pyridine	Notes
RM31	1.0 ml	0.5 ml	0.5 ml	1 ml	-	0.8 ml	hemi-pentahydrate used 80ºC for 24hrs

Alterations to both the solvents and the ligands employed were recorded as trials RM 59.2-63.2. While not significant in antimicrobial effectiveness, single crystal data is still being acquired to determine the novelty of several of these structures.

Table 3 - Trials Exchanging DMF and Ethanol

Vial	M/L	M (in DMF)	L (in DMF)	DMF	EtOH	Pyridine	Notes

59.2	1ml	0.5ml in DMSO	0.5ml in DMSO	1ml DMSO	-	0.1ml	Exchange DMF for DMSO and Ethanol for DI H2O Ligand Chelidamic acid
60.2	1ml	0.5ml in DMSO	0.5ml in DMSO	0.5ml DMSO	0.5ml H2O	0.1ml	Exchange DMF for DMSO and Ethanol for DI H2O Ligand Chelidamic acid
61.2	1ml	0.5ml in DMSO	0.5ml in DMSO	-	1ml H2O	0.1ml	Exchange DMF for DMSO and Ethanol for DI H2O Ligand Chelidamic acid
62.2	1ml	0.5ml in H2O	0.5ml in H2O	0.5ml DMSO	0.5ml H2O	0.1ml	Exchange DMF for DMSO and Ethanol for DI H2O Ligand Chelidamic acid
63.2	1ml	0.5ml in H2O	0.5ml in H2O	-	0.5ml H2O	0.1 ml	Exchange DMF for DMSO and Ethanol for DI H2O Ligand Chelidamic acid

RM116 was run at ambient room temperature, approximately 28ºC. It employed a 1.5:0.5 DMF:Ethanol solvent ratio, and exchanged the 0.1ml of pyridine for 0.08mmol of sulfapyridine.

Table 4 - Trial 116, Sulfapyridine Integrated Crystal

Vial	M/L	M (in DMF)	L (in DMF)	DMF	EtOH	Sulfonamide	Notes
116	1.0 ml	0.5 ml	0.5 ml	0.5ml	0.5 ml	0.08mmol sulfapyridine	40ºC for 24hrs
117	1.0 ml	0.5 ml	0.5 ml	0.5 ml	0.5 ml	0.04mmol sulfapyridine	40ºC for 24hrs

The last significant runs to speak on were those evaluating the adhesive potential of metal-organic frameworks to different surfaces. The initial trials are displayed in Table 5 below.

Table 5 - Trials For Surface Adhesion Properties

Vial	M/L	M (in DMF)	L (in DMF)	DMF	EtOH	Pyridine	Notes
46	1ml	0.5ml	0.5ml	0.5ml	0.5ml	0.1ml	Ligand is 0.04mmol 3,5-H_2PDC Minimal adhesion to glass
47	1ml	0.5ml	0.5ml	0.5ml	0.5ml	0.4ml	Ligand is .04mmol 3,5-H2PDC No adhesion to glass
48	1ml	0.5ml	0.5ml	0.5ml	0.5ml	0.8ml	Ligand is .04mmol 3,5-H2PDC No adhesion to glass
49	1ml	0.5ml	0.5ml	0.5ml	0.5ml	0.1ml	Ligand is .04mmol 3,5-H2PDC 46 repeat for implant trial, limited adhesion to implant observed
50	1.0 ml	0.5 ml	0.5 ml	0 ml	1.0 ml	0.1 ml	RM1, testing growth on glassware Minimal adhesion to glass

At this point it was proposed that greater adhesion may be observed if the reactions were run at room temperature. The results of these trials are as follows -

Table 6 - Continued Trials For Surface Adhesion

Vial	M/L	M (in DMF)	L (in DMF)	DMF	EtOH	Pyridine	Notes
55	1ml	0.5ml	0.5ml	0.5ml	0.5ml	.8ml	Ligand is .04mmol 3,5-H2PDC Repeat 48 Adheres exceptionally well to glass
56	1ml	0.5ml	0.5ml	0.5ml	0.5ml	.1ml	Ligand is .04mmol 3,5-H2PDC
57	1ml	0.5ml	0.5ml	0.5ml	0.5ml	.4ml	Ligand is .04mmol 3,5-H2PDC Repeat 47 room temp Adheres very well to glass
58	1ml	0.5ml	0.5ml	0.5ml	0.5ml	.8ml	Ligand is .04mmol 3,5-H2PDC Repeat 48 room temp, testing with implant Adheres very well to glass

For all crystal products, after production the sample was cleaned to remove the leftover starting materials through a series of solvent washes. The initial wash reproduced the conditions of the solvent bath the crystals were formed in (mother solution/liquer). This ratio was gradually increased to 100% ethanol, due to the evaporation rates of ethanol.

For biological testing, blood agar media was used to encourage the hemolytic properties of *S.mutans.* To standardize bacterial concentration, *S. mutans* was grown overnight and then added to sterile saline solution until a McFarland value of 0.5 or OD600 value of 0.08-0.1 was achieved. Then, 200μL were pipetted on to the blood agar plate and a 3-direction streak was performed. 0.01g of each framework was added, as well as the corresponding mass amounts of each reagent. For example, 0.01g of RM1 contains 24μmol of Cu^{2+}, which corresponds to 0.001489g. The plates were placed in a 37^{o}C oven to mimic biological temperatures and left for 24 hours. After that period, the results were evaluated. Zones of inhibition were calculated based on radius.

IV. Results / Discussion

The initial focus of this project was to find ideal conditions to generate pure phases of RM1 and RM2, and to verify the purity of these structures using a variety of analytical techniques. The comprehensive data illustrating the effectiveness of purification can be seen in the figures below-

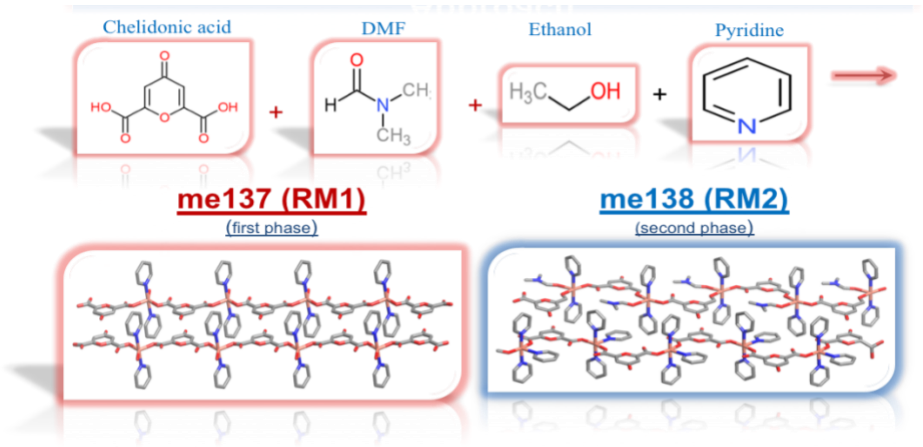

Figure 1. Reaction scheme for RM1 and RM2, respectively.

Analyzing the frameworks above, there are several features that are noteworthy. RM1 presents a trigonal bipyramidal structure, where the coppers are connected by the branching ligand chelidonic acid. Each copper employs three terminal ligands, two are pyridine and one water. RM2 likewise employs copper branched by chelidonic acid, but it features a square pyramidal geometry. Additionally, this framework is composed of two different units which generate alternating chains. One chain is functionalized with three pyridines as terminal ligands, while the other is functionalized by two pyridines and one DMF. Table 1 in the materials and methods section is the third set of trials for generating RM1 and RM2, and it was not until the fourth set of trials that the conditions were properly standardized. The most important alteration to ensuring the purity of the yields was to sonicate the reagents when adding them to the solvent solutions to ensure their homogenous distribution. It was also seen through the initial trials that the order of the addition of reagents played a role in the crystal formation, and that the time of incubation at 85°C also had an impact on the yield. However, the exact implication of these factors is not fully understood yet, and further trials are being performed modifying these conditions to determine this. To confirm the purity of the fourth round of trials, the crystal products were analyzed using PXRD. To analyze their thermal stability, TGA analysis was performed.

Figure 2 below illustrates the experimental PXRD data for the third trial of RM1 (noted here as RM3.4) plotted against the known spectrum for this crystal product, referred to as me137. While there are some differences in magnitude of observed peaks, this was not a concerning observation, as this can be related to solvent and preferred orientation. The alignment of the peaks and the presence of no extra peaks were both important features, and this indicated the successful experimental production of me137. PXRD analysis is based on x-ray diffraction, and the amplitude of observed peaks is dependent on orientation of crystals. Consequently, the amplitude of the peaks will be different with every test.

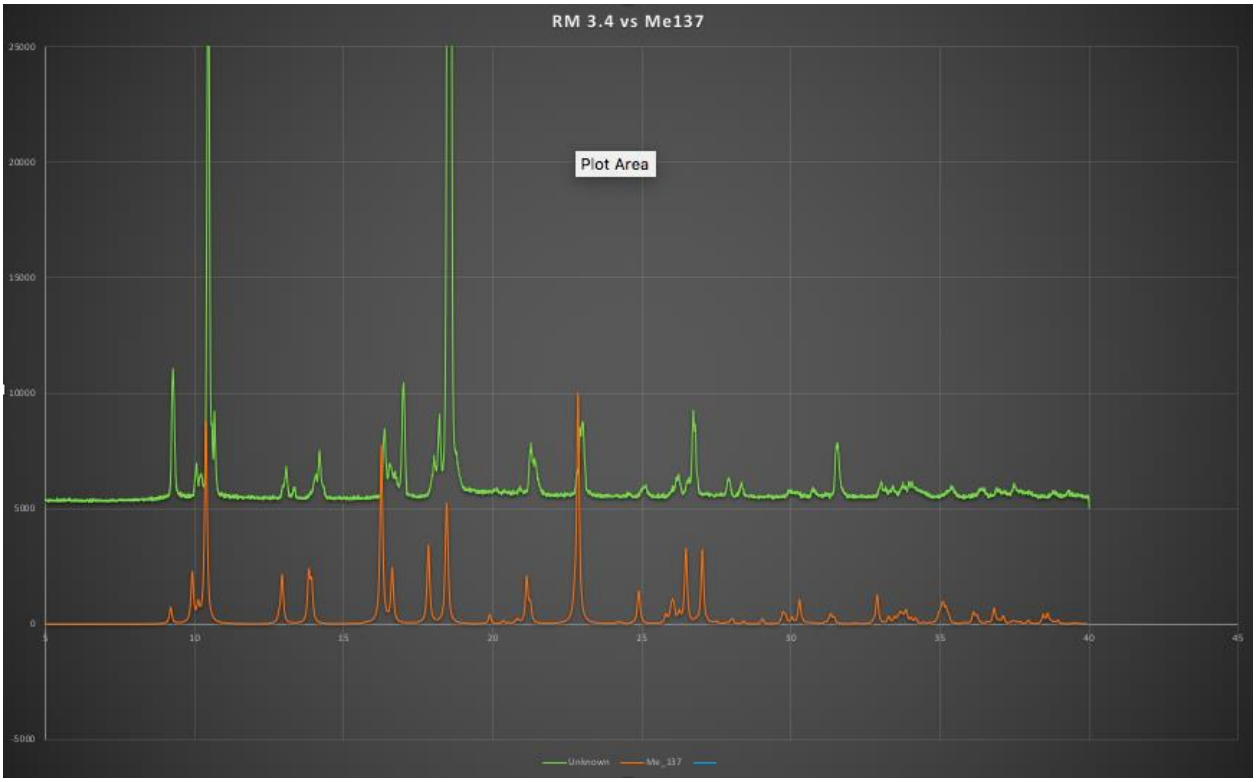

Figure 2. PXRD data of RM1 before ethanol wash
Green: experimental and orange: simulated

Figure 3 illustrates the PXRD data of RM1 after washing with ethanol, while Figure 4 illustrates RM1 (once again noted as RM3.4) after one week suspended in an ethanol solution. These spectra both illustrate that the structure maintained its integrity. This data was also confirmed through visual observations, with the crystals appearing to maintain their integrity when observed microscopically (e.g., no cracks, loss or rounding of edges, or discoloration).
Seeing that this structure could be produced and then purified, it was decided to scale up the reaction amounts to provide more mass of product and test the conditions to ensure stability was maintained. When produced in 5x the initial volume, with direct fivefold expansions in the mass of reagents and volume of solvents, the PXRD data again illustrated the effective production of RM1.

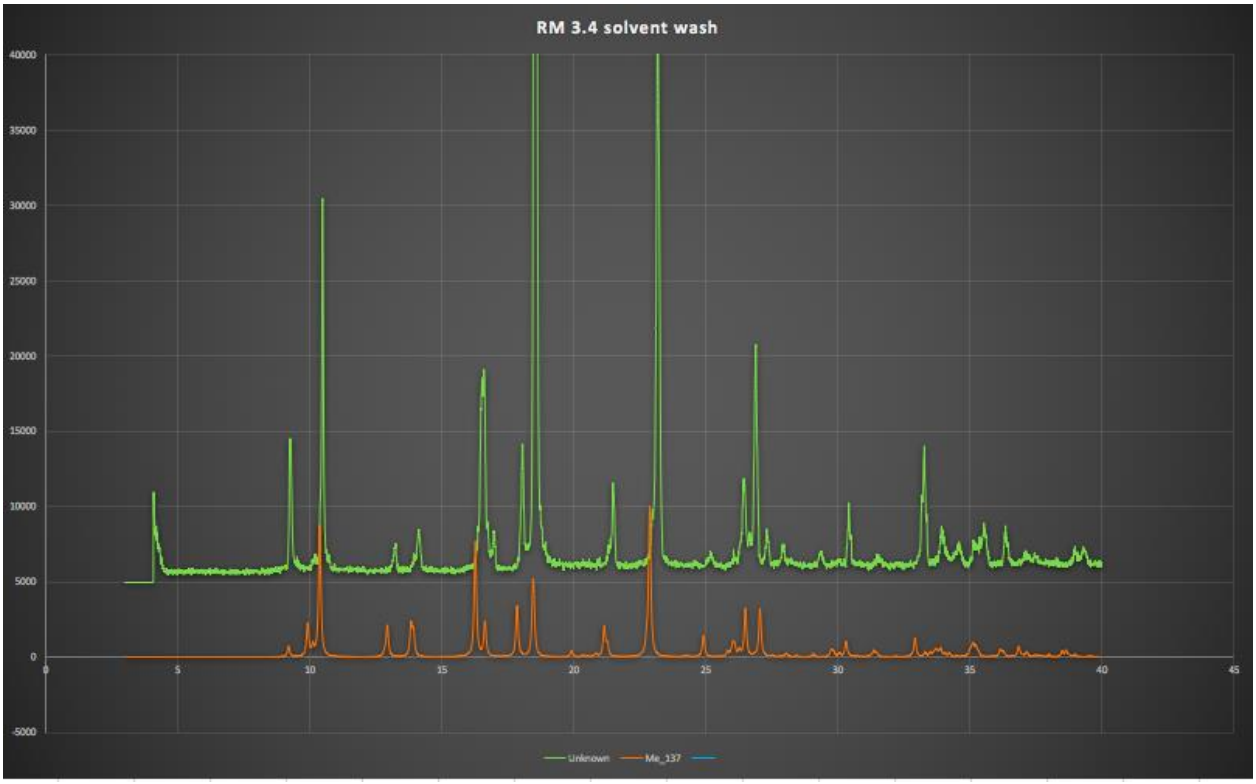

Figure 3. PXRD data of RM1 after ethanol wash
Green: experimental and orange: simulated

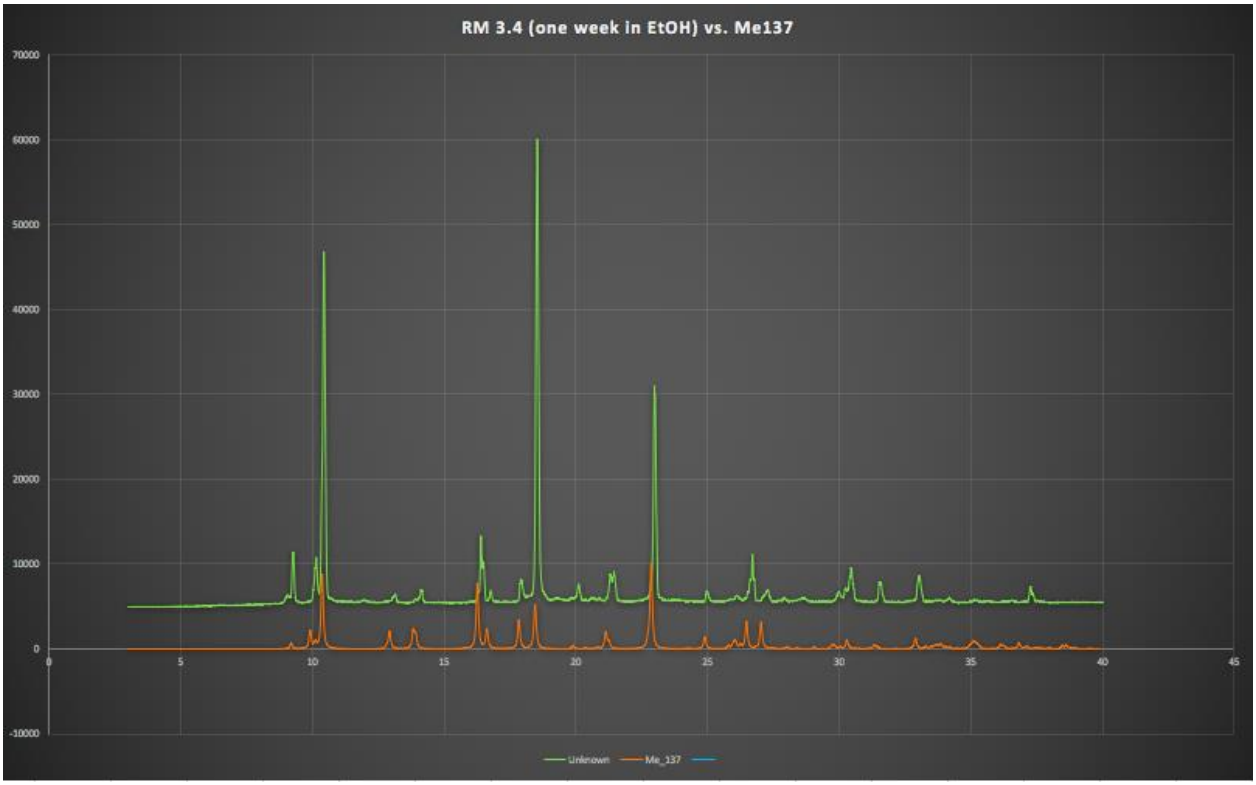

Figure 4. PXRD data of RM1 after one week in EtOH
Green: experimental and orange: simulated

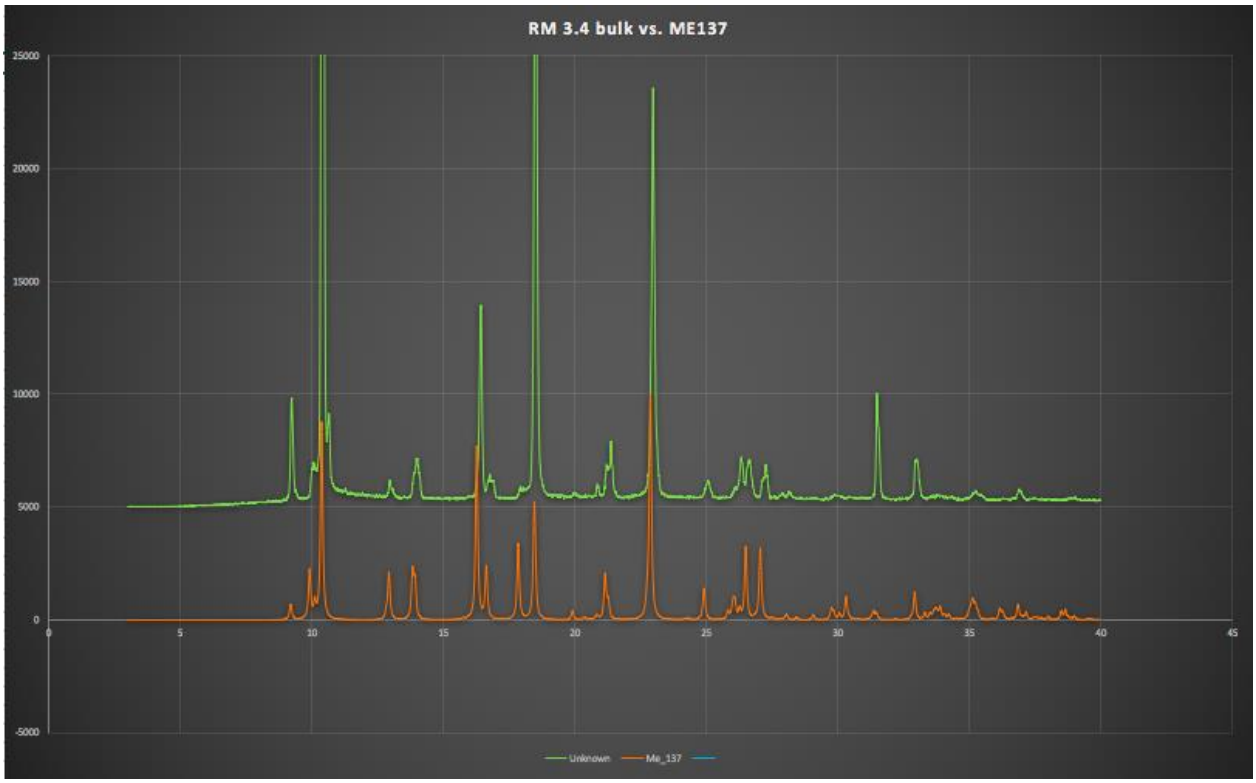

Figure 5. PXRD data of 5x increased volume RM1, as-synthesized (i.e., before solvent wash)
Green: experimental and orange: simulated

One additional method of analysis, TGA, was performed. This method illustrates the weight lost at different temperatures while heating the structure, in this case, up to 800 ℃. Observing the TGA data from Figure 6 below, approximately 5% of the structure weight was lost at 125°C. This temperature range corresponded to the temperature range for conjugated H_2O, which was used to in mass calculations and could be used to reinforce diffraction data collected from the PXRD. With the structure of RM1 as $[Cu_1CDO_1\ pyr_2\ H_2O]_n$, the structural molecular weight is 423.95g/mol. With H_2O weighing 18.1g/mol, it is 4.3% of the overall molecular weight. This corresponds to our approximation of 5% water that was obtained during TGA analysis, which supports the production of RM1.

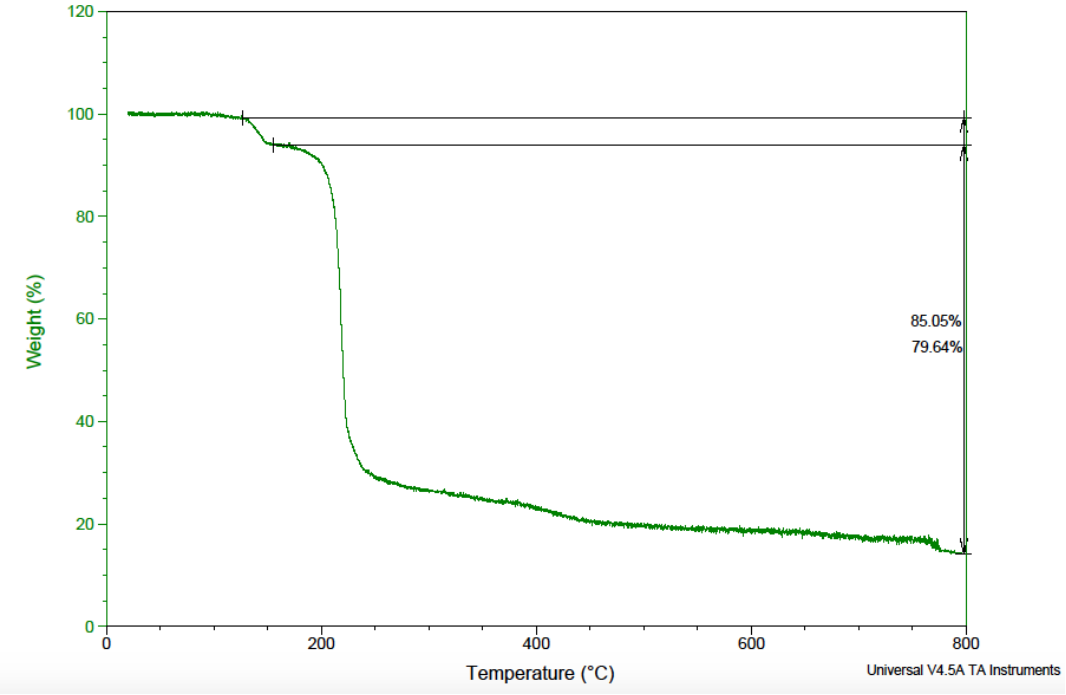

Figure 6. TGA data for RM1

At this point, another important discovery was made regarding framework stability. When in solution, RM1 and RM2 retain their structural stability incredibly well. However, as soon as RM2 is removed from solution, the crystals transition phase to RM1. This process has been verified by repetitive PXRD runs, as well as the color transition observed in Figure 7 below.

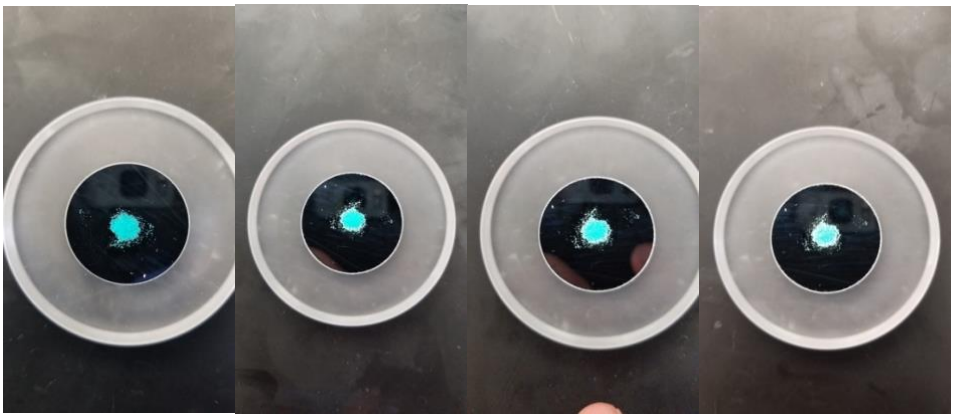

Figure 7. Transformation of RM2 to RM1

Because these frameworks have the potential to photodimerize when exposed to UV conditions, it was reasonable to assume that exposure to the X-ray via PXRD was at least partially responsible for the observed transition. To assess the validity of this prediction, RM2 was produced, removed from solution, and left exposed to the lab environment for 24hrs. The results can be seen below in Figure 8 below.

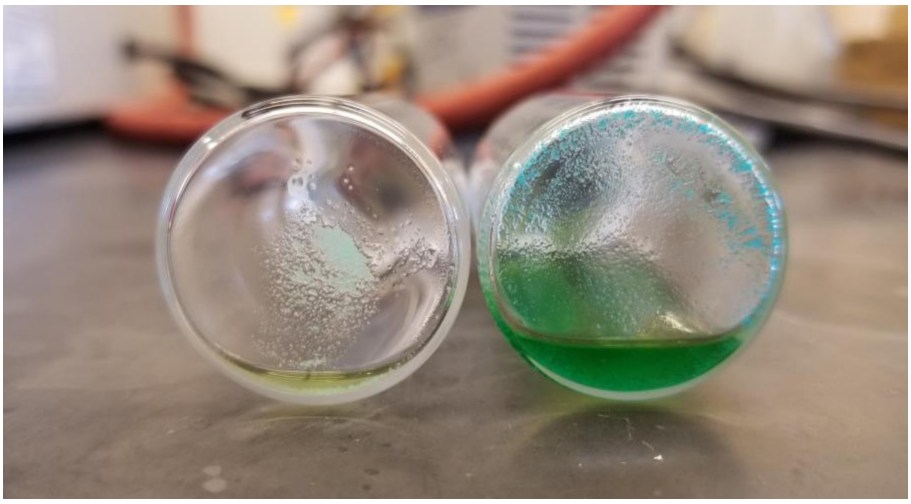

Figure 8. Transformation of RM2 to RM1 at Ambient Conditions

With these results, it was confirmed that the crystal was transitioning phases as a consequence of removal from solution. It was hypothesized that this transition was occurring as a consequence of the humid environment in lab, which was exposing the structures to H_2O. Despite the anticipated higher binding affinity of copper to nitrogen, the exposure to H_2O somehow resulted in the removal of a pyridine or DMF substituent depending on the RM2 chain in question, causing it to revert to RM1. To test this hypothesis, it was proposed that pyridine be employed to varying degrees of excess (from 0.2ml-1ml, increasing in 0.2ml increments). Because it was thought that water was responsible for the transition, oversaturating the solution with pyridine would theoretically result in the expulsion of water from the framework. Considering the binding affinity of copper for nitrogen (such as those present on pyridine) it would be likely that this would inhibit water from being able to reach and integrate with the structure. The excess pyridine had no impact on structure, until the threshold of 0.8ml was reached. At this point, the following structure (RM31) was generated –

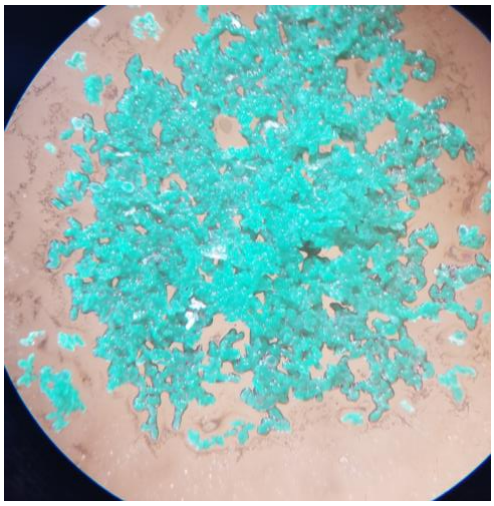

Figure 9. Crystal Product RM31

Initially thought to be RM2, the PXRD was taken to verify phase and crystallinity. The results, however, disagreed with our expectations. As seen in the PXRD below, RM31 was neither RM1 or RM2.

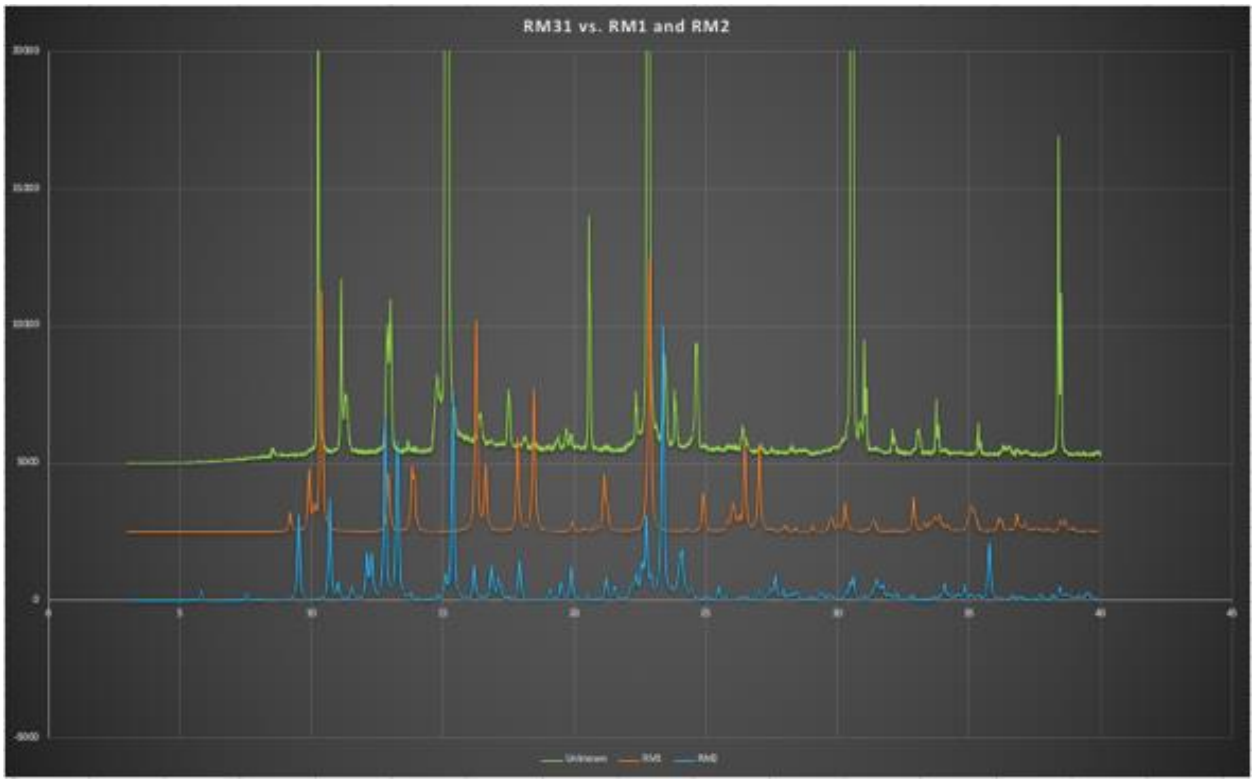

Figure 10. PXRD data of RM31
Blue: RM2, Orange: RM1, Green: RM31 (unknown)

The product appeared to be a new phase, so it was sent for single crystal analysis. The results verified this theory, indicating that the product was composed of the unit observed in the figure below.

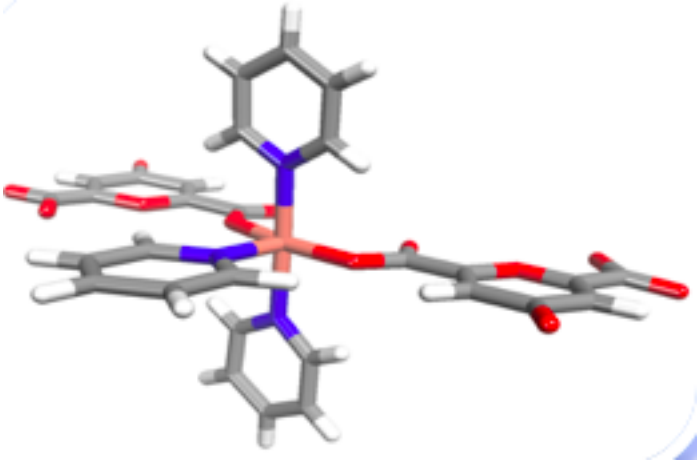

Figure 11. Unit Cell of RM31

The unit cell may look familiar, because it is one of the two repeating units of RM2. Essentially, oversaturating the solution with pyridine resulted in the removal of DMF from one of the chains, exchanging it with pyridine. Despite this structural change, RM31 reverted back to RM1. The transformation of RM2 to RM1 occurred within as little as 5 minutes, while the transformation of RM31 to RM1 required up to 45 minutes depending on room conditions. At this point, an additional control was employed to ensure that water was responsible for the phase transition. The conditions for RM1 and RM2 were utilized, but 100µl of DI H_2O was added to each reaction. In all cases, RM1 was produced independently of variations in solvent ratios. The products of these runs, as seen in Figure 12, were verified to be identical through PXRD. Even prior to this analysis though, it can be seen that visually they are identical. The only difference being the amount of product produced in each vial, with RM129 having the most crystals and RM131 having the least.

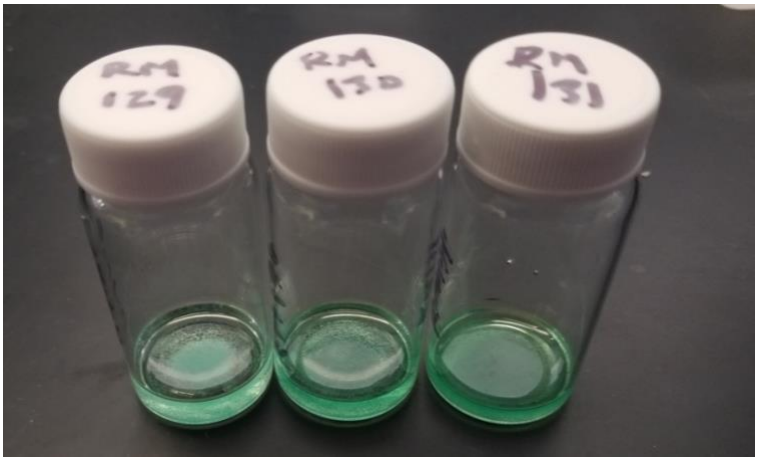

Figure 12. RM1 and RM2 Conditions With 100µl of DI H_2O

This led to the conclusion that the phase transition must be a consequence of interactions with water in the humid environment. Nonetheless, a controllable single crystal transformation is fairly unique and merited further investigation.

The next question was whether or not it was a reversible transition that was occurring. The RM2 and RM31 crystals were left out for 24hours, and then placed in solutions with increasing concentrations of pyridine. In a solution of pure pyridine, a visible transition occurred with the light blue/green RM1 crystals becoming significantly darker in color, indicated by RV1 (revert1) which can be seen in Figure 10 below.

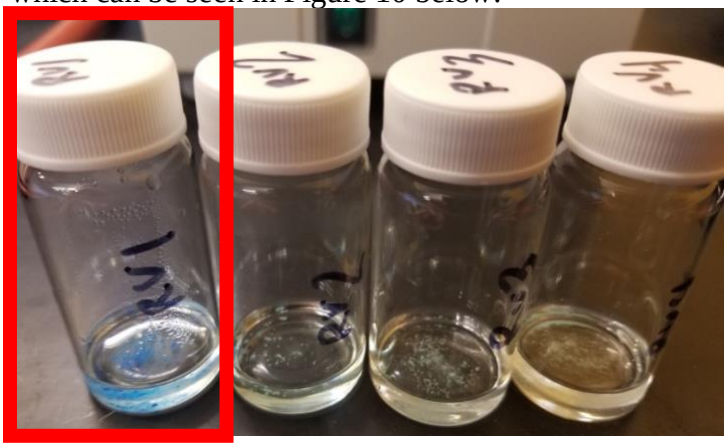

Figure 13. Transition of RM1, With Variations in Pyridine Concentration

The RM1 used in these trials had more powder like character than crystallinity, as it had been crushed to be employed in bacterial testing. With that in mind, a PXRD was still attempted to identify the phase of the new product. This PXRD is seen as Figure 14 below.

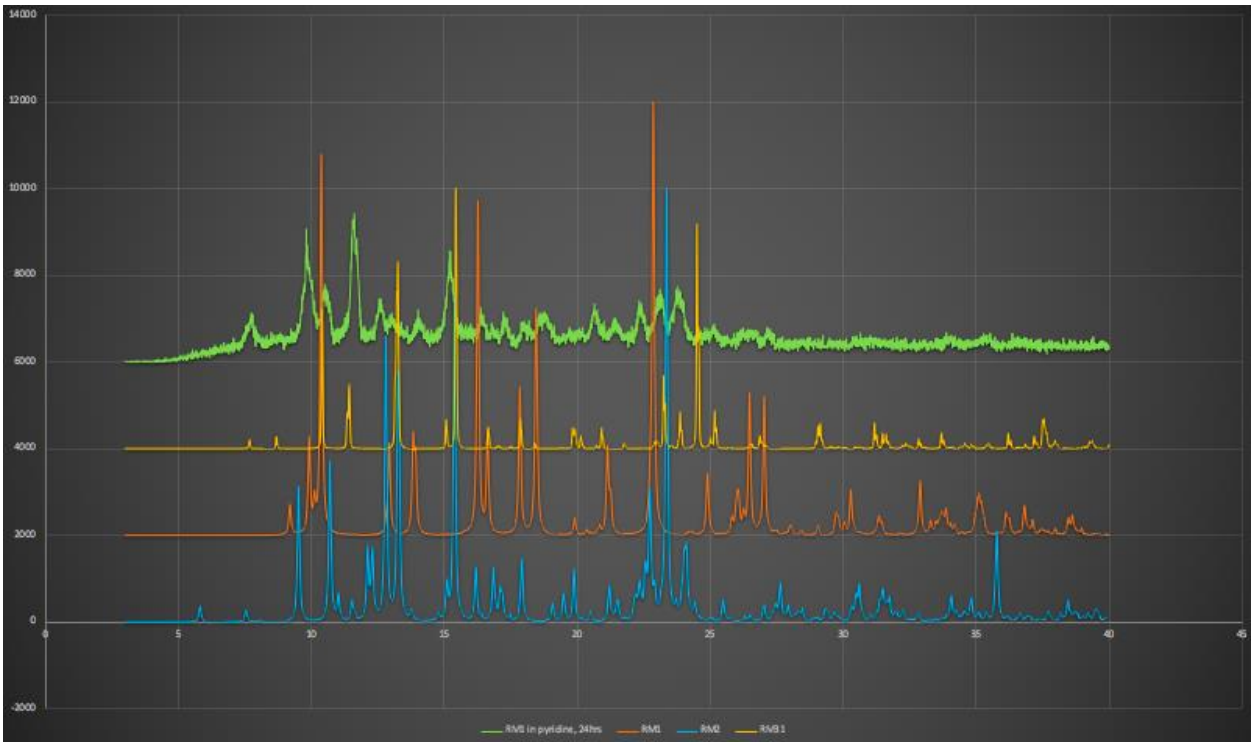

Figure 14. PXRD data of RV1 Unknown Identification
From bottom to top, the powder patterns in this graphic are RM2, RM1, RM31, and the unknown in question (identified as RV1).

As anticipated, the unknown powder pattern has a much lower degree of crystallinity than the other three. Looking at the overlapping peaks, it is possible that the observed product has character of both RM2 and RM31. However, to draw any distinct conclusions it will be necessary to conduct this trial again with product that has a much higher degree of crystallinity. The rationale behind this claim is that crystalline products are more highly ordered and have less surface area available for reactions to take place. This may result in a slower transition between phases, which could be producing an intermediate phase. Additionally, a more crystalline product would result in a PXRD with a lower background noise, also providing more definitive results.

At this point, it was decided to move forward in to biological testing with RM1 and RM31. The rationale here was that the phase transition, while interesting, only had an effect on this project if the frameworks illustrated antimicrobial properties. RM31 was employed because its transition was delayed for almost an hour, whereas RM2 was removed as its transition occurred too rapidly. Antimicrobial effectiveness was evaluated by employing a Kirby-Bauer zone of inhibition test. This test was performed as discussed in the Biemer et.al. article.[24] and elaborated on in the materials and methods section above. The results are displayed below.

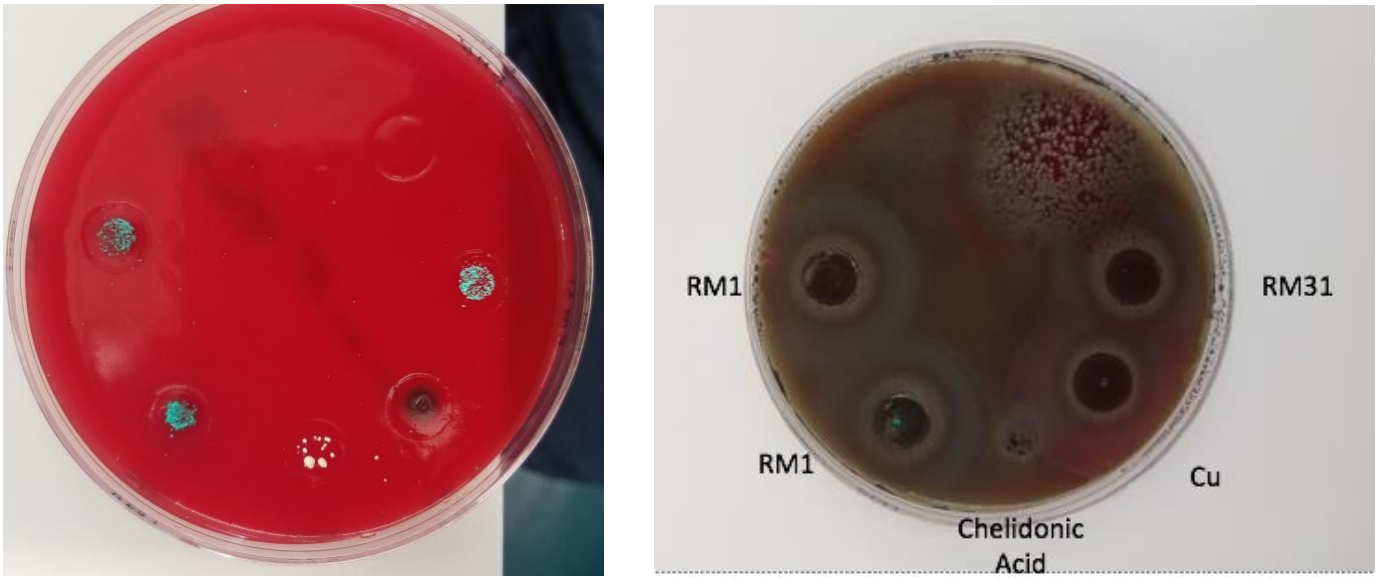

Figure 15. 24 Hour Plate, Biological Testing of Framework Antimicrobial Effectiveness

These results presented a number of interesting conclusions. Most importantly, it appeared that the copper is the component of these frameworks that was responsible for the antimicrobial effect of the framework, while chelidonic acid contributed minimally if at all. With this in mind, it is not surprising that the inhibition seen by all three compounds was almost the same as copper alone.

While these results were frustrating, they presented avenues for further exploration. After reviewing the work done in the 2016 Borthagaray et. al. article, it was decided to work with three different sulfonamides which did not contain a five membered heterocycle.[18] As they were unable to validate these structures as effectively more antimicrobial when complexed with metal ions, it presented an avenue for additional scientific discovery if synergistic inhibition could be generated.

While the sulfonamides were being shipped, it was decided to study the effectiveness of ligands similar to chelidonic acid for structure formation and then, hopefully, for antimicrobial effectiveness. One particular ligand, chelidamic acid, was investigated significantly. This ligand was chosen for several of reasons - it was structurally very similar to chelidonic acid and it was readily available. Additionally the nitrogen on chelidamic acid was noted to have antiviral effects, particularly in targeting HIV, and it would be interesting to investigate and evaluate its antimicrobial effectiveness as well. The first trial, RM51, produced no crystal precipitates. This was suspected to be a consequence of tautomerization in the chelidamic acid functional group. Literature suggested that altering the solvents to vary polarity could favor the formation of one tautomer over the other, so a series of reactions were performed exchanging DMF for DMSO and ethanol for water. These trials can be seen in Table 3 of the materials and methods section. The “x.2” designation is because trials 59-63,which were supposed to be these exact trials, were performed using chelidonic acid instead of chelidamic. Of the chelidonic acid trials, seen below, three were effective in producing crystals which have been sent for single crystal analysis. These were trials 60, 62 and 63.

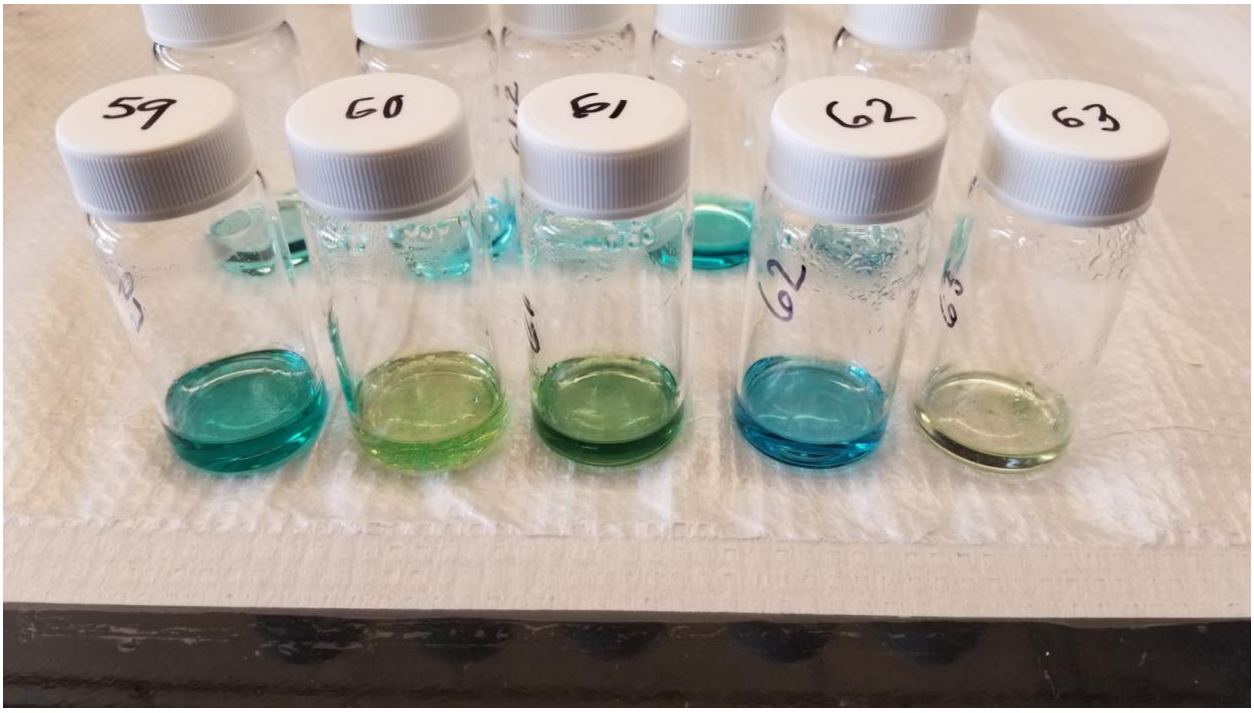

Figure 16. Series of Trials Exchanging DMF and Ethanol For DMSO and Water

Of the chelidamic acid trials seen below, only 63.2 was effective at producing crystals which have also been sent for single crystal analysis. This validates the literature based assumptions regarding the shift in polarity of solvents being able to influence the tautomerization of chelidamic acid.

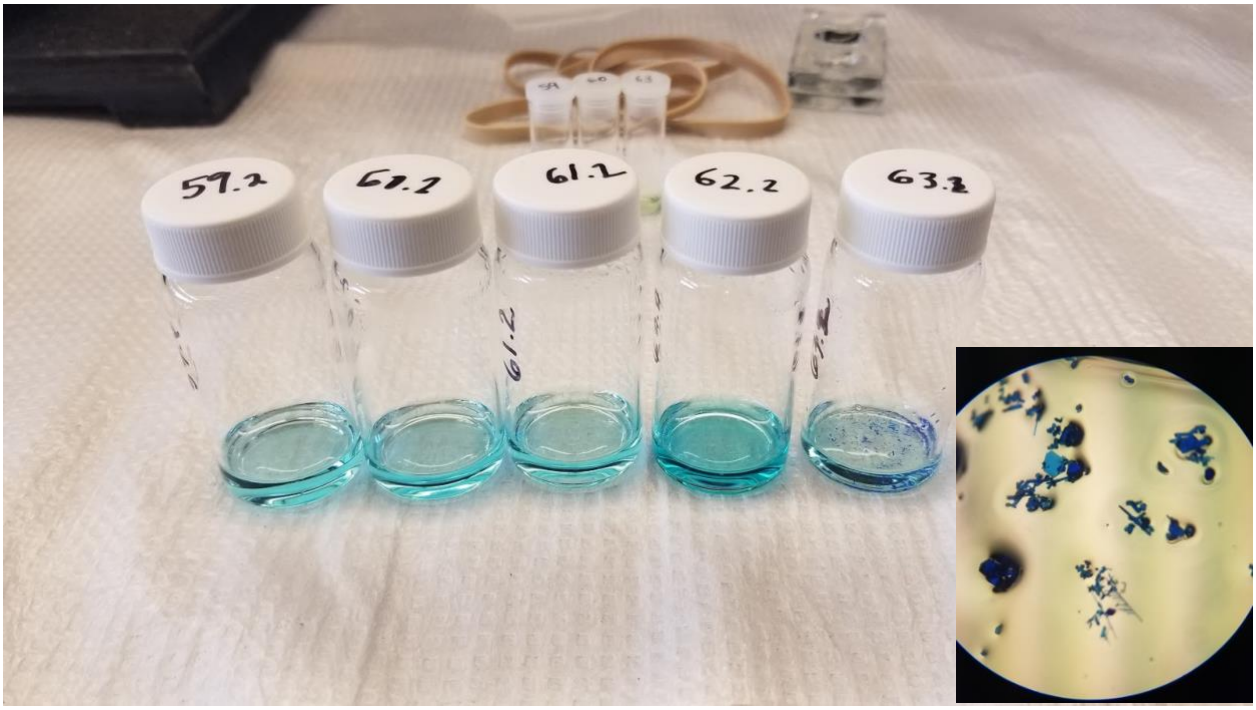

Figure 17. Series of Trials Exchanging Chelidonic Acid for Chelidamic Acid, DMF and Ethanol For DMSO and Water, Including Magnified view of RM63.2

At this point the sulfonamide compounds that were purchased arrived, so the focus shifted from chelidamic acid testing back to sulfonamides while waiting for single crystal data. The compounds purchased were sulfapyridine, sulfamerazine, and sulfadiazine, which can be seen below -

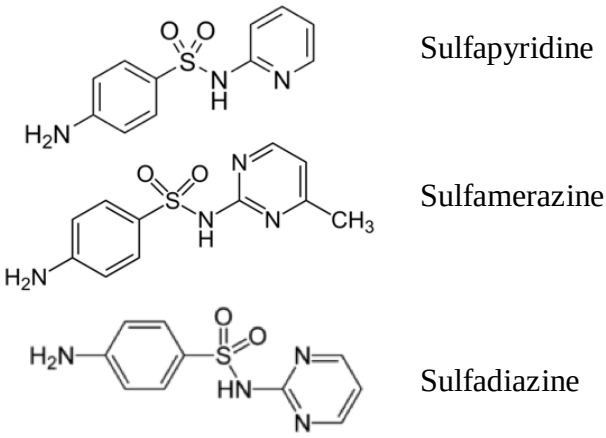

Sulfapyridine

Sulfamerazine

Sulfadiazine

Figure 18. Sulfonamides Employed For Ligand Exchange

These particular ligands were chosen for several reasons. First, they each employ six membered heterocycles rather than five membered ones. Secondly, each of these compounds could be easily, and cheaply obtained. Lastly, these compounds are structurally very similar. The expectation was that these could be exchanged with pyridine on the generated RM1 and RM2 frameworks, so having structural similarities to pyridine could be hugely beneficial to this end. The conditions employed directly mimicked those of RM1, with the exception of pyridine being replaced by sulfapyridine. Ideally, this would result in sulfonamide integration at the place of pyridine as seen in the figure below –

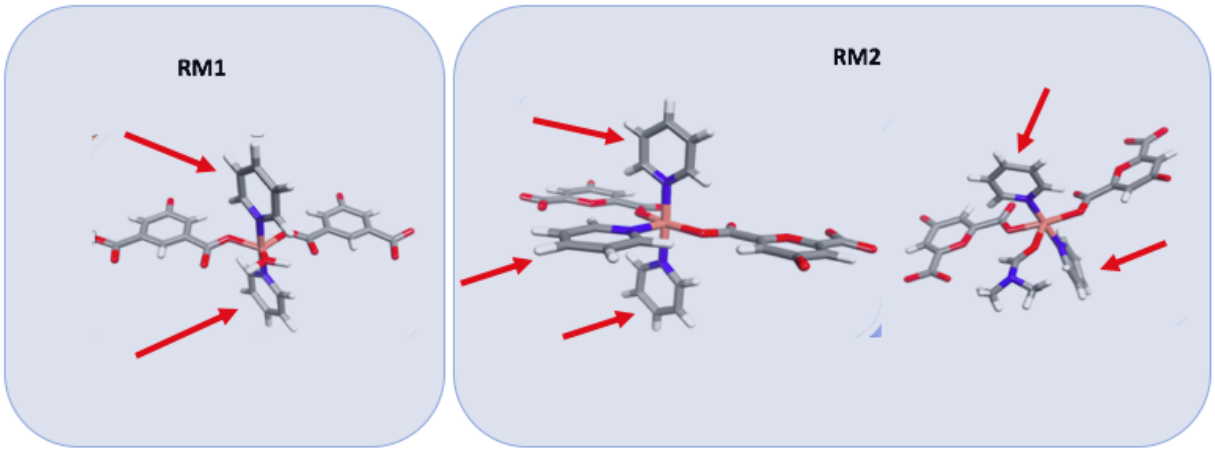

Figure 19. Anticipated Integration Points of Sulfonamides on RM1 and RM2

With the exchange of pyridine for sulfapyridine, it was anticipated that it would occupy the newly available terminal ligand spaces. Run RM116 was the first successful trial with sulfapyridine, and its conditions are displayed in the materials and methods section above. To highlight the key attributes, it employed a 1.5:0.5 DMF:Ethanol ratio and exchanged the 0.1ml of pyridine for 0.08mmol of sulfapyridine. Additionally, this run was performed at 40°C for 24 hours. The reduction of temperature was necessary, as higher temperature runs were producing microcrystals or no crystals at all. The physical crystalline product is displayed in Figure 20 below.

Figure 20. RM116 Crystalline Product

This product produced crystals which were sent for single crystal analysis, although the results of that test have not been received yet. With that data, it could be determined if the actual crystal structure matches the theoretical one proposed previously.
Prior to obtaining single crystal data, IR was used to evaluate whether or not sulfapyridine was present in the RM116 structure. After this determination, antimicrobial testing could progress before obtaining single crystal results. The spectra of RM116, compared to that of sulfapyridine, can be seen below.

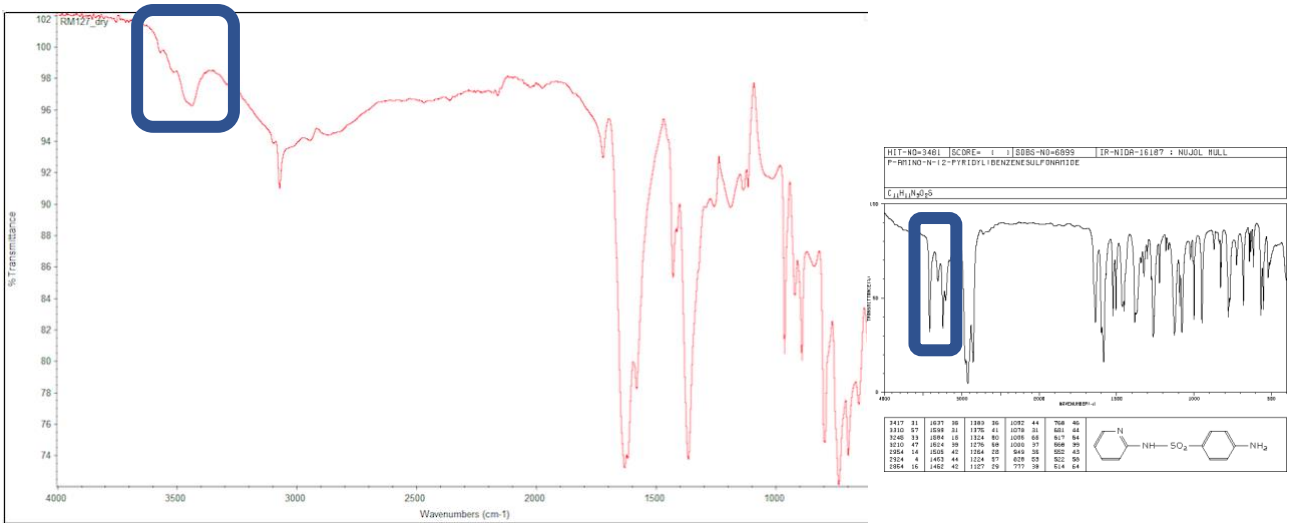

Figure 21. IR of RM116 in Comparison With Sulfapyridine

Standard spectra for sulfapyridine obtained from ebiochemicals.com[25]

While there are lots of overlaps between sulfapyridine and the metal-organic framework structure, one unique region is above 3500cm^{-1}. In this range, highlighted above, is where peaks for primary amines appear. With the presence of the multiplet in this region, it was assumed that sulfapyridine was responsible and consequently integrated into the RM116 framework. It is also of note that this IR was performed on a dry sample. In this case, dry implies that the sample was washed with the solvent bath it is synthesized in (ie. Mother solution), then washed with ethanol and left to dry.

With the confirmation of sulfapyridine in the structures, the next step was biological testing. Once again a Kirby-Bauer zone of inhibition test was performed, and the results can be observed below.

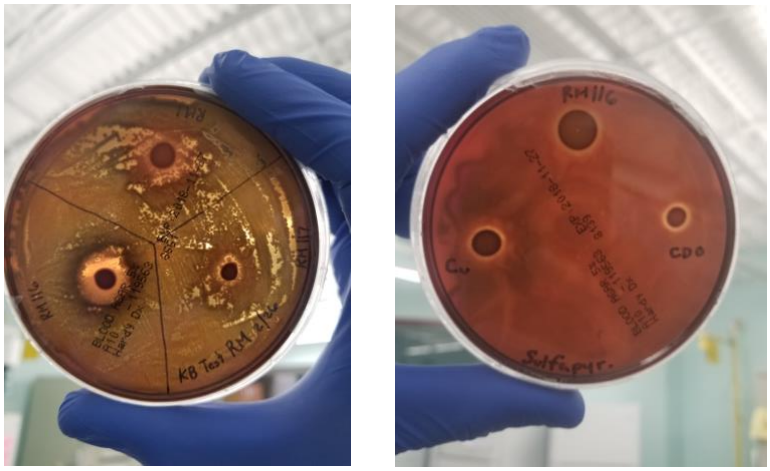

Figure 22. Biological Testing of RM116/117

To determine whether the new structures improved upon RM1, they were first tested against it. As seen in the above figure, RM116 illustrated a significantly larger zone of inhibition than either RM117 or RM1. In light of this, RM116 was tested against each of its solid reagents (Copper, chelidonic acid, and sulfapyridine) where it presented as more effective than copper or chelidonic acid independently. However, sulfapyridine created no observable zone of inhibition whatsoever. This result was unexpected, and explorations of literature yielded minimal insights. One particular publication had complexes with sulfapyridine and elected to solubilize them in DMF and produce stock solutions, which weree diluted accordingly and added to Mueller Hinton Agar (Difco) previously melted and cooled to 40 °C for the preparation of antibiotic plates. This agar was distributed onto Petri dishes so as to obtain sulfapyridine concentrations of 8, 16, 32, 64, 96, 128, 193, 257, 385, 513 and 1,027 µM.[26] This procedure could be employed in future tests, as it would allow for the solubilization of sulfapyridine in DMF.

While the focus of this project was to develop antimicrobial frameworks, it was more specifically to develop antimicrobial frameworks that could be grown on dental implants. Throughout the inhibition trials, there was also investigation into the adhesion of these frameworks to titanium surfaces of implants. Several dental implants were acquired from a local practitioner and were used for this study. Initially, the growth of frameworks was evaluated both

on titanium and on glass. The framework that was used exchanged the chelidonic acid ligand for a 0.04mmol 3,5-H_2PDC ligand. This structure was noted by Dr. Eubank to have strong adhesive properties in previous research, so it would serve as a good foundation for testing the growth of frameworks on different surfaces. The first set of trials, displayed in Table 5 in the materials and methods section, were relatively ineffective at achieving adhesion.
As observed in Table 6 of the materials and methods section, reducing the reaction to be run at room temperature proved to be hugely beneficial in generating crystal product. The products of runs RM55,56,57,and 58 can be seen below.

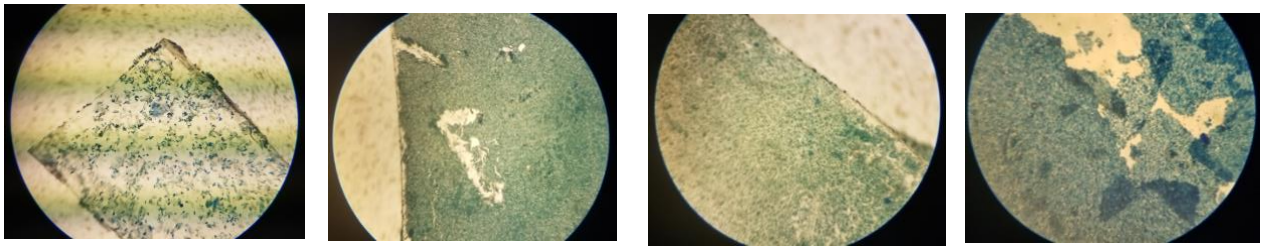

Figure 23. Crystal Products of RM55, RM56, RM57 and RM58 From Left to Right

These trials presented crystals that were significantly more effective at adhering to glass and titanium surfaces. RM55, the most successful at generating strong adhesion, was then employed in testing on dental implants. The growth of the frameworks on the titanium implant can be seen below -

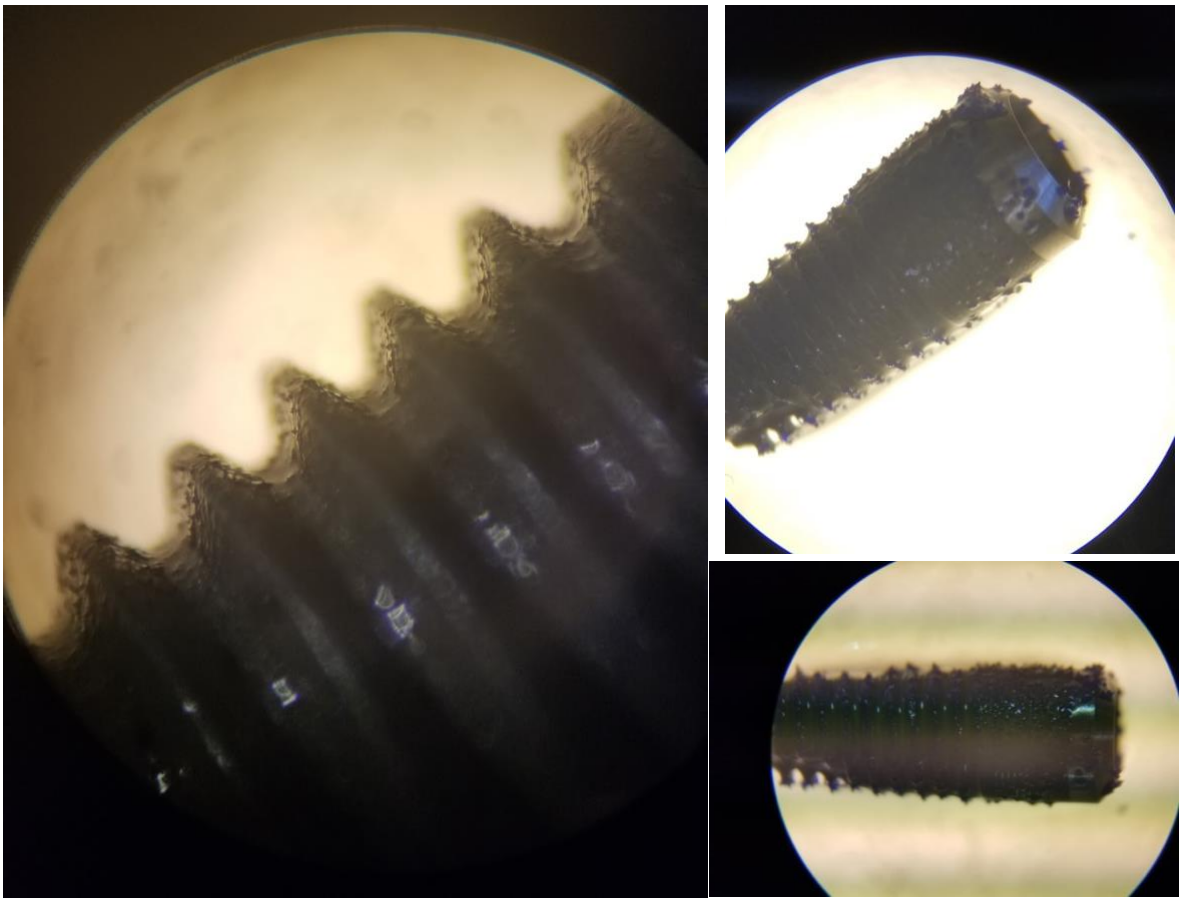

Figure 24. Adhesion of Frameworks to Titanium Dental Implant

As seen in the image above, the crystals attached do appear to be microcrystalline in nature. Further testing will be required to determine whether their growth is uniform or not, as well as whether or not crystal size can me modulated. For example, SEM could be employed to observe the degree of crystallinity as well as the uniformity of their growth. Additionally, testing should be performed to determine the strength of adhesion. Data regarding this at the moment is purely qualitative, and quantitative results would further support the argument for strong adhesion.

V. Conclusion

The purpose of this project was to develop antimicrobial metal-organic frameworks which would adhere to dental implants and inhibit *S.mutans* binding. Beginning with the synthesis of RM1 and RM2, both were able to be produced and characterized. However, the phase transition of RM2 to RM1 delayed the progression in to biological testing. The focus shifted to the mechanism behind this transition and potential modifications to prevent it from occurring. In doing this, a novel framework (RM31) was discovered. While it still transitioned to RM1, it had increased stability and was able to be employed in biological testing. The results of this initial testing illustrated the ineffectiveness of these frameworks as antimicrobial agents, but allowed for exploration in to potential modifications to increase the efficacy of their bacterial inhibition. While the introduction of chelidamic acid was overall ineffective, the incorporation of sulfonamides was significantly better. Despite still waiting on single crystal results, it is believed that a sulfapyridine-integrated framework (RM116) was generated which illustrated an

exponentially larger zone of inhibition than its individual reagents. Because of the late development of this product, there is significant further testing needed to validate these results. Furthermore, additional testing is needed to study the potential growth of RM116 on dental implant surfaces. The work done with implant adhesion in this study, despite only employing Cu frameworks with the 3,5-H_2PDC ligand, illustrates the potential for framework adhesion to these implants and presents an avenue for further study.

In regards to future studies, there are many directions for additional development. First, while antimicrobial effectiveness of RM116 was observed it needs to be validated. Copper may have a role in hemolysis and consequently inhibit bacteria that are exclusively hemolytic through this mechanism, but in doing so it does not actually attack and kill the bacteria. Testing with different medias and bacteria should be employed to ensure that the mechanism of action is the desired one. Additionally, the effect of sulfapyridine, or lack thereof, needs to be further evaluated. It would be suggested to employ the procedure of Marzano et. Al.[26] in future studies to solubilize the framework as well as sulfapyridine and to establish more accurate results in terms of inhibition. Aside from this testing, future work could evaluate the mechanism behind the phase transformation of RM2 and RM31. Computational studies could help to model this transition, and better RM1 crystal product could be used to suspend in pyridine. Doing this would allow for better PXRD results, which could be used to characterize the unknown product referred to as RV1 in this report. In addition, work could be done evaluating adhesion to dental implants. The work done in this project supports the claim that lower temperature runs yield better products, which may make RM116 an ideal framework for adhesion. While all of these proposed ideas further develop the work conducted in this study, there are also new avenues which could expand on the work done here. In 2013, Gao et. al. published on the effects of different wavelength UV photofunctionalization on micro-arc oxidized titanium. Essentially, they discovered that UV treatment of dental implant surfaces enhances bioactivity and osseointegration by altering the titanium dioxide on the surface.[10] While there is limited published data on this focus, it would be interesting to see what impact UV light has on the antimicrobial properties of different frameworks, if at all.

References

(1) Papathanasiou, E.; Finkelman, M.; Hanley, J.; Parashis, A. O. Prevalence, Etiology and Treatment of Peri-Implant Mucositis and Peri-Implantitis: A Survey of Periodontists in the United States. *J. Periodontol.* **2016**, *87* (5), 493–501. https://doi.org/10.1902/jop.2015.150476.

(2) Okayasu, K.; Wang, H.-L. Decision Tree for the Management of Periimplant Diseases. *Implant Dent.* **2011**, *20* (4), 256–261. https://doi.org/10.1097/ID.0b013e3182263589.

(3) Heitz-Mayfield, L. J. A.; Mombelli, A. The Therapy of Peri-Implantitis: A Systematic Review. *Int. J. Oral Maxillofac. Implants* **2014**, *29 Suppl*, 325–345. https://doi.org/10.11607/jomi.2014suppl.g5.3.

(4) Chan, H.-L.; Lin, G.-H.; Suarez, F.; MacEachern, M.; Wang, H.-L. Surgical Management of Peri-Implantitis: A Systematic Review and Meta-Analysis of Treatment Outcomes. *J. Periodontol.* **2014**, *85* (8), 1027–1041. https://doi.org/10.1902/jop.2013.130563.

(5) Paju, S.; Scannapieco, F. A. Oral Biofilms, Periodontitis, and Pulmonary Infections. *Oral Dis.* **2007**, *13* (6), 508–512. https://doi.org/10.1111/j.1601-0825.2007.01410a.x.

(6) Quirynen, Marc, D. S., Marc. Infectious risks for oral implants: a review of the literature - Quirynen - 2002 - Clinical Oral Implants Research - Wiley Online Library https://onlinelibrary.wiley.com/doi/pdf/10.1034/j.1600-0501.2002.130101.x (accessed Apr 23, 2019).

(7) Persson, G. R.; Samuelsson, E.; Lindahl, C.; Renvert, S. Mechanical Non-Surgical Treatment of Peri-Implantitis: A Single-Blinded Randomized Longitudinal Clinical Study. II. Microbiological Results. *J. Clin. Periodontol.* **2010**, *37* (6), 563–573. https://doi.org/10.1111/j.1600-051X.2010.01561.x.

(8) Faveri, M.; Figueiredo, L. C.; Shibli, J. A.; Pérez-Chaparro, P. J.; Feres, M. Microbiological Diversity of Peri-Implantitis Biofilms. In *Biofilm-based Healthcare-associated Infections: Volume I*; Donelli, G., Ed.; Advances in Experimental Medicine and Biology; Springer International Publishing: Cham, 2015; pp 85–96. https://doi.org/10.1007/978-3-319-11038-7_5.

(9) Prathapachandran, J.; Suresh, N. Management of Peri-Implantitis. *Dent. Res. J.* **2012**, *9* (5), 516–521.

(10) Gao, Y.; Liu, Y.; Zhou, L.; Guo, Z.; Rong, M.; Liu, X.; Lai, C.; Ding, X. The Effects of Different Wavelength UV Photofunctionalization on Micro-Arc Oxidized Titanium. *PLOS ONE* **2013**, *8* (7), e68086. https://doi.org/10.1371/journal.pone.0068086.

(11) Wuttke, S.; Zimpel, A.; Bein, T.; Braig, S.; Stoiber, K.; Vollmar, A.; Müller, D.; Haastert-Talini, K.; Schaeske, J.; Stiesch, M.; et al. Validating Metal-Organic Framework Nanoparticles for Their Nanosafety in Diverse Biomedical Applications. *Adv. Healthc. Mater.* **2017**, *6* (2), 1600818. https://doi.org/10.1002/adhm.201600818.

(12) Horcajada, P.; Gref, R.; Baati, T.; Allan, P. K.; Maurin, G.; Couvreur, P.; Férey, G.; Morris, R. E.; Serre, C. Metal–Organic Frameworks in Biomedicine. *Chem. Rev.* **2012**, *112* (2), 1232–1268. https://doi.org/10.1021/cr200256v.

(13) Giménez-Marqués, M.; Hidalgo, T.; Serre, C.; Horcajada, P. Nanostructured Metal–Organic Frameworks and Their Bio-Related Applications. *Coord. Chem. Rev.* **2016**, *307*, 342–360. https://doi.org/10.1016/j.ccr.2015.08.008.

(14) Bhardwaj, N.; Pandey, S. K.; Mehta, J.; Bhardwaj, S. K.; Kim, K.-H.; Deep, A. Bioactive Nano-Metal–Organic Frameworks as Antimicrobials against Gram-Positive and Gram-Negative Bacteria. *Toxicol. Res.* **2018**, *7* (5), 931–941. https://doi.org/10.1039/C8TX00087E.
(15) Lu, X.; Ye, J.; Zhang, D.; Xie, R.; Bogale, R. F.; Sun, Y.; Zhao, L.; Zhao, Q.; Ning, G. Silver Carboxylate Metal–Organic Frameworks with Highly Antibacterial Activity and Biocompatibility. *J. Inorg. Biochem.* **2014**, *138*, 114–121. https://doi.org/10.1016/j.jinorgbio.2014.05.005.
(16) Aguado, S.; Quirós, J.; Canivet, J.; Farrusseng, D.; Boltes, K.; Rosal, R. Antimicrobial Activity of Cobalt Imidazolate Metal–Organic Frameworks. *Chemosphere* **2014**, *113*, 188–192. https://doi.org/10.1016/j.chemosphere.2014.05.029.
(17) Wyszogrodzka, G.; Marszałek, B.; Gil, B.; Dorożyński, P. Metal-Organic Frameworks: Mechanisms of Antibacterial Action and Potential Applications. *Drug Discov. Today* **2016**, *21* (6), 1009–1018. https://doi.org/10.1016/j.drudis.2016.04.009.
(18) Borthagaray, G. Essential Transition Metal Ion Complexation as a Strategy to Improve the Antimicrobial Activity of Organic Drugs.
(19) Kremer, E.; Facchin, G.; Estévez, E.; Alborés, P.; Baran, E. J.; Ellena, J.; Torre, M. H. Copper Complexes with Heterocyclic Sulfonamides: Synthesis, Spectroscopic Characterization, Microbiological and SOD-like Activities: Crystal Structure of [Cu(Sulfisoxazole)2(H2O)4]·2H2O. *J. Inorg. Biochem.* **2006**, *100* (7), 1167–1175. https://doi.org/10.1016/j.jinorgbio.2006.01.042.
(20) Centrone, A.; Yang, Y.; Speakman, S.; Bromberg, L.; Rutledge, G. C.; Hatton, T. A. Growth of Metal−Organic Frameworks on Polymer Surfaces. *J. Am. Chem. Soc.* **2010**, *132* (44), 15687–15691. https://doi.org/10.1021/ja106381x.
(21) Li, W.; Meng, Q.; Li, X.; Zhang, C.; Fan, Z.; Zhang, G. Non-Activation ZnO Array as a Buffering Layer to Fabricate Strongly Adhesive Metal–Organic Framework/PVDF Hollow Fiber Membranes. *Chem. Commun.* **2014**, *50* (68), 9711–9713. https://doi.org/10.1039/C4CC03864A.
(22) Rubin, H. N.; Neufeld, B. H.; Reynolds, M. M. Surface-Anchored Metal–Organic Framework–Cotton Material for Tunable Antibacterial Copper Delivery. *ACS Appl. Mater. Interfaces* **2018**, *10* (17), 15189–15199. https://doi.org/10.1021/acsami.7b19455.
(23) Eubank, J. F.; Kravtsov, V. Ch.; Eddaoudi, M. Synthesis of Organic Photodimeric Cage Molecules Based on Cycloaddition via Metal−Ligand Directed Assembly. *J. Am. Chem. Soc.* **2007**, *129* (18), 5820–5821. https://doi.org/10.1021/ja070924n.
(24) Biemer, J. J. Antimicrobial Susceptibility Testing by the Kirby-Bauer Disc Diffusion Method. *Ann. Clin. Lab. Sci.* **1973**, *3* (2), 135–140.
(25) Sulfapyridine IR 144-83-2 2-Sulfapyridine; 4-((2-Pyridylamino)sulfonyl)aniline; 4-amino-N-(2-pyridinyl)benzenesulfonamide; 4-amino-N-(pyridin-2-yl)benzenesulfonamide eBiochemicals https://www.ebiochemicals.com/Wiki/QcEB000012784_IR_2.html (accessed Apr 23, 2019).
(26) Marzano, I. M.; Franco, M. S.; Silva, P. P.; Augusti, R.; Santos, G. C.; Fernandes, N. G.; Bucciarelli-Rodriguez, M.; Chartone-Souza, E.; Pereira-Maia, E. C. Crystal Structure, Antibacterial and Cytotoxic Activities of a New Complex of Bismuth(III) with Sulfapyridine. *Molecules* **2013**, *18* (2), 1464–1476. https://doi.org/10.3390/molecules18021464.